Geologia USP
Série Científica

DOI: 10.11606/issn.2316-9095.v18-124101

Revista do Instituto de Geociências - USP
Geol. USP, Sér. cient., São Paulo, v. 18, n. 3, p. 3-13, Setembro 2018

Petrophysical characterization of coquinas from Morro do Chaves Formation (Sergipe-Alagoas Basin) by X-ray computed tomography

Caracterização petrofísica das coquinas da Formação Morro do Chaves (Bacia de Sergipe-Alagoas) utilizando a tomografia computadorizada de raios X

Aline Maria Poças Belila[1], Michelle Chaves Kuroda[1],
João Paulo da Ponte Souza[2], Alexandre Campane Vidal[2], Osvair Vidal Trevisan[1]
[1]Departamento de Engenharia do Petróleo, Faculdade de Engenharia Mecânica, Universidade Estadual de Campinas - UNICAMP, Rua Mendeleyev, 200, CEP 13083-860, Cidade Universitária Zeferino Vaz, Barão Geraldo, Campinas, SP, BR
(belila@dep.fem.unicamp.br; mckuroda@gmail.com; trevisan@dep.fem.unicamp.br)
[2]Departamento de Geologia e Recursos Naturais, Instituto de Geociências, UNICAMP, Campinas, SP, BR
(joao.ponte.souza@gmail.com; vidal@dep.fem.unicamp.br)

Received on December 13, 2016; accepted on June 08, 2018

Abstract

Carbonate rocks constitute a large number of petroleum reservoirs worldwide. Notwithstanding, the characterization of these rocks is still a challenge due to their high complexity and pore space variability, indicating the importance of further studies to reduce uncertainty in reservoir interpretation and characterization. This work was performed for coquina samples from Morro do Chaves Formation (Sergipe-Alagoas Basin), analogous to important Brazilian reservoirs. Computed tomography (CT) was used for three-dimensional characterization of rock structure. The neural network self-organizing maps (SOM) was used for CT images segmentation. According to our tests, CT demonstrated to be a consistent tool for quantitative and qualitative analysis of heterogeneous pore space, by the evaluation of porosity, connectivity and the representative elementary volume.

Keywords: Coquinas; X-ray computed tomography; Petrophysics; Representative elementary volume.

Resumo

As rochas carbonáticas constituem um grande número de reservatórios de petróleo no mundo, contudo a caracterização dessas rochas ainda é um desafio em virtude de sua alta complexidade e da variabilidade do espaço poroso, indicando a importância de novos estudos para reduzir a incerteza associada à interpretação e caracterização dos reservatórios carbonáticos. Este trabalho foi realizado para amostras de coquinas da Formação Morro do Chaves — Bacia de Sergipe-Alagoas —, rochas análogas a importantes reservatórios brasileiros. A tomografia computadorizada (TC) de raios X foi empregada para a caracterização tridimensional da estrutura da rocha. A rede neural Self-Organizing Maps (SOM) foi utilizada para a segmentação das imagens tomográficas. De acordo com nossos testes, a TC demonstrou ser uma ferramenta consistente para a análise qualitativa e quantitativa de espaços porosos heterogêneos, avaliando a porosidade, a conectividade e o volume elementar representativo.

Palavras-chave: Coquinas; Tomografia computadorizada de raios x; Petrofísica; Volume elementar representativo.

INTRODUCTION

Carbonate reservoirs are characterized by high heterogeneity and structural complexity, which may reflect the high variability of facies and diagenetic processes resulting in a system with high unpredictability (Lucia, 2007). The pore space is directly related to rock heterogeneity, exhibiting a variety of porosity types and poor correlation with other rock properties (Lonoy, 2006).

Therefore, there are several works aiming the pore space characterization in carbonates rocks by using different laboratory techniques, such as traditional petrographic analysis, capillary pressure, X-ray computed tomography (CT) and magnetic resonance imaging (Vogel and Brown, 2003; Vincent et al., 2011; Hulea and Nicholls, 2012).

By using CT, it is possible to render porosity from a sample volume, revealing the pore sizes and shapes while also allowing for investigating heterogeneity. The advance in tomographic data interpretation is associated with the application of image analysis methods, making it possible to quantify several rock parameters (Ketcham and Carlson, 2001; Van Geet et al., 2003; Vik et al., 2013).

The combination of CT data with traditional petrographic analysis becomes an effective methodology for the study of carbonate rocks regarding porosity and diagenetic features (Okabe and Blunt, 2007; Reis Neto et al., 2011). Petrography is important to connect CT results to geological features and reduce mistakes in interpretation.

Furthermore, another important aspect that can be investigated in CT images is the definition of an appropriate sample support that encompasses rock heterogeneity. In this way, the advantage of using CT is not only the pore space characterization, but also that the porosity values in different volumes can be compared and a reliable sample size can then be quantified (Razavi et al., 2007; Al-Raoush and Papadopoulos, 2010; Fernandes et al., 2012).

Therefore, the goal of the present work is the petrophysical characterization of coquinas from Morro do Chaves Formation focused on the analysis of representative elementary volume (REV) for the main porosity types. For this purpose, the rock characterization is performed using petrographic descriptions and CT analysis.

MATERIALS AND METHODS

The rocks from Morro do Chaves Formation are composed of shell beds deposited on detrital accumulations and associated with carbonate platforms (Figueiredo, 1981). Sedimentary structures indicate the transport and deposition by storm events (Castro, 1988; Azambuja Filho et al., 1998). These rocks, also called *coquinas*, occur in the eastern Brazilian margin and western Africa associated with a lacustrine system of the rift basin stage during the opening of the Atlantic Ocean in the Early Cretaceous and can be considered analogous to some reservoirs in the Campos and Santos Basin.

Cimpor quarry, located in the city of São Miguel dos Campos,Alagoas, was chosen for the study of coquinas from Morro do Chaves Fm, Sergipe-Alagoas Basin. The fieldwork was carried out aiming the main lithofacies identification and sampling. From the collected samples, four of them were selected based on the classification of Lucia (1983) to represent the different petrophysical behaviors. Figure 1 shows the workflow used for sample characterization.

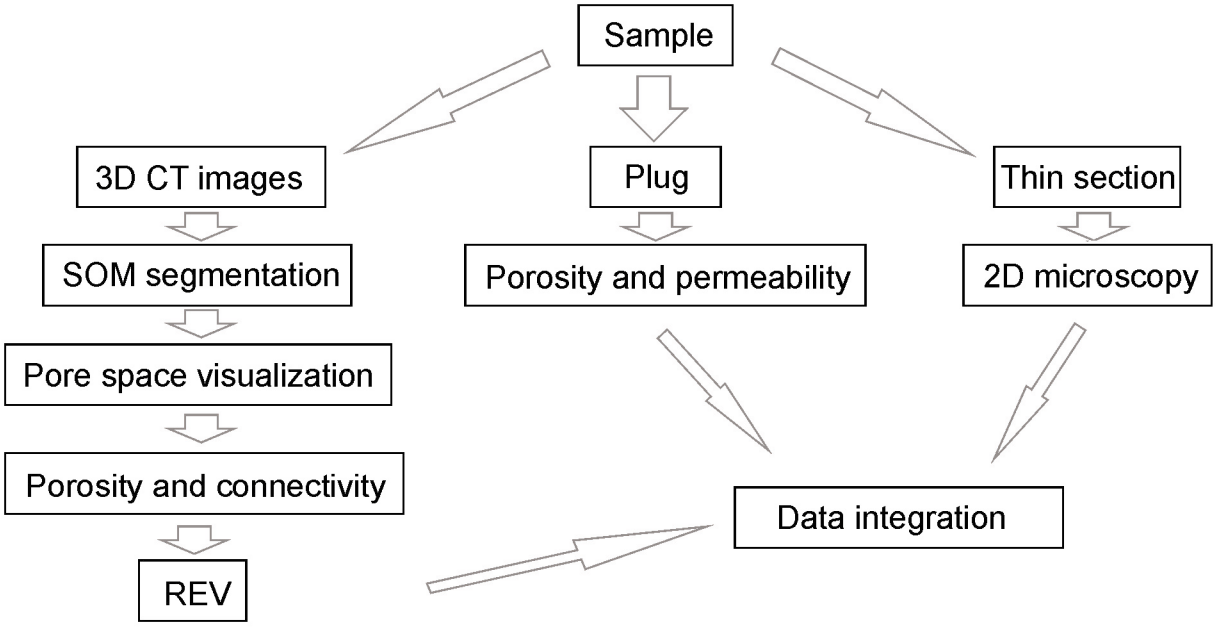

CT: computed tomography; SOM: self-organizing maps; REV: representative elementary volumes: 2D: two dimensions.

Figure 1. Flowchart representing the work routine used for samples characterization.

A Siemens industrial tomography device, model SWFVD30C, was used for image acquisition, at the Center for Petroleum Studies of the University of Campinas (Cepetro/ Unicamp). By using this device, only pores larger than 0.2 mm could be identified. At this resolution, it was possible to scan samples larger than 30 cm in order to assess the appropriate volume to represent rock heterogeneity, which is especially important in vuggy carbonates.

One of the main uses of CT in reservoir characterization is the study of petrophysical properties. Nevertheless, before carrying out the petrophysical analysis, it is necessary to segment the images by separating them in rock and pore regions. There are many techniques usually used to segment three-dimensional (3D) CT images, such as the image thresholding by indicator kriging (Oh and Lindquist, 1999), the piecewise constant level set method (Lie et al., 2006), the Ridler and Calvard method (Ridler and Calvard, 1978), Otsu threshold method (Otsu, 1979) and the edge based kriging segmentation algorithm (Arns et al., 2005).

In order to segment the 3D CT images, the neural network self-organizing maps (SOM) was used. Two of the advantages of SOM are being a non-supervised technique of segmentation and it does not require prior information for data set classification. Therefore, this tool is adaptable to different types of data and assists the characterization of data with absence or scarcity of information (Kohonen, 2001; Bhatt and Helle, 2002; Arzuman, 2009). SOM has been successfully used in many scientific fields, such as geology, engineering and medicine. Li and Chi (2005) and Mei et al. (2017) show the use of SOM for brain images segmentation. Besides, Coléou et al. (2003) describes the advantage of using SOM compared to other multivariate statistical techniques such as P*rincipal* C*omponent* A*nalysis (*PCA), Independent Component Analysis (ICA) and K-means. More details of SOM technique and the algorithm parameters settings can be found in Kohonen (2001).

Regarding the segmented images, for evaluating rock connectivity, an algorithm to calculate the volume of connected pores from the total porosity, which is equivalent to the effective porosity, was also applied. The algorithm was developed in C++ and it compares the value of a central point with its neighbors, establishing a relationship between them based on the intensity values of each point and then defining the connected pores throughout the rock.

After segmentation, concerning the petrophysical analysis, it is essential that the sample support encompasses the pore space heterogeneity. The minimum volume required for a reliable analysis can be defined by the REV (Bear, 1972).

To delimit the REV, measurements are made on a block that is continuously divided into subvolumes until values of mean and variance remain constant or stationary (Corbett and Jensen, 1992; Tidwell and Wilson, 1997; Nordahl and Ringrose, 2008).

The variography was also used as geostatistical parameter to assess rock heterogeneity. Variograms are commonly used in petrophysical analysis to define the variable spatial continuity in different directions, which is controlled by geological factors (Lucia and Fogg, 1990; Wang et al., 1994; Sahin et al., 1998).

To simplify the application of the connectivity algorithm and also the REV calculations, samples were cut into the volume of interest (VOI), which is defined by the maximum parallelepiped inside the sample.

In order to validate the method presented in this paper, plugs of 1" in diameter were produced to calculate porosity and permeability by gas injection (nitrogen). For it, we have used the UltraPore Porosimeter and UltraPerm Gas Permeameter (Core Laboratories, Amsterdam).

The basic petrography was performed in transmitted light using a polarizing microscope, aiming the description of textural components, porosity types and diagenetic modifiers.

RESULTS AND DISCUSSION

Sample data and classification

The samples consist of coquinas formed predominantly by bioclasts of pelecypod bivalve, with sizes ranging from less than 1 to 15 mm. The samples were classified as calcarenites and calcirudites, according to Grabau's classification (Grabau, 1904). The classification was based on the detrital origin of coquina samples, which is evident from its fragmentation, transport and deposition. Samples have little or no carbonate matrix and significant percentage of siliciclastic matrix and grains.

By using CT images and petrographic analysis, it was possible to identify a wide variety of pore sizes, shapes and distributions, which are directly related to the petrophysical properties. According to Lucia (1983), samples were classified based on their porosity types (Figure 2). The author has compared the rock fabric with petrophysical properties in carbonates and proposed a pore space classification based on groups with similar petrophysical behaviors, recognizing the importance of different pore types:

- *interparticle* for pores located between grains or crystals;
- *separate vugs* for pores located within grains, or pores significantly larger (typically two times larger) than the particles and connected only by interparticle porosity;
- *touching vugs* for pores significantly larger than the particles, located between grains or crystals, that are interconnected by other vugs.

The porosity types are associated to the diagenetic processes occurring after the rock burial. The cement dissolution is the main controlling factor in the actual porosity. Interparticle porosity is associated with cement dissolution in the intergranular space and also in the contact between the crystals (Figures 2A and 2B). The sample with separate vugs shows dissolution inside the grains, creating isolated pores (Figure 2C). The touching vugs are related both to cement dissolution and fracturing system, exhibiting connection pathways throughout the rock (Figure 2D).

Computed tomographic images

SOM algorithm was used to define a porosity threshold for each sample, separating the CT images into two sets (pore and rock phases) (Figure 3). The images are composed of voxels that represent average measurements of small regions in the rock. The voxel size depends on the spatial resolution of CT. The relatively low resolution of CT (0.2 mm) explains the Gaussian shape of the histograms in Figure 3. Due to the *partial volume effect* each voxel may contain not only pore or grain, but also a mix of them, thus creating an average intensity value that hinders segmentation, making the use of computational techniques, such as SOM, necessary, to reduce uncertainty in this process (Ketcham and Carlson, 2001).

The porosity values obtained by image segmentation were very close to the values obtained in the plugs by gas injection. Besides, the effective porosity (percentage of

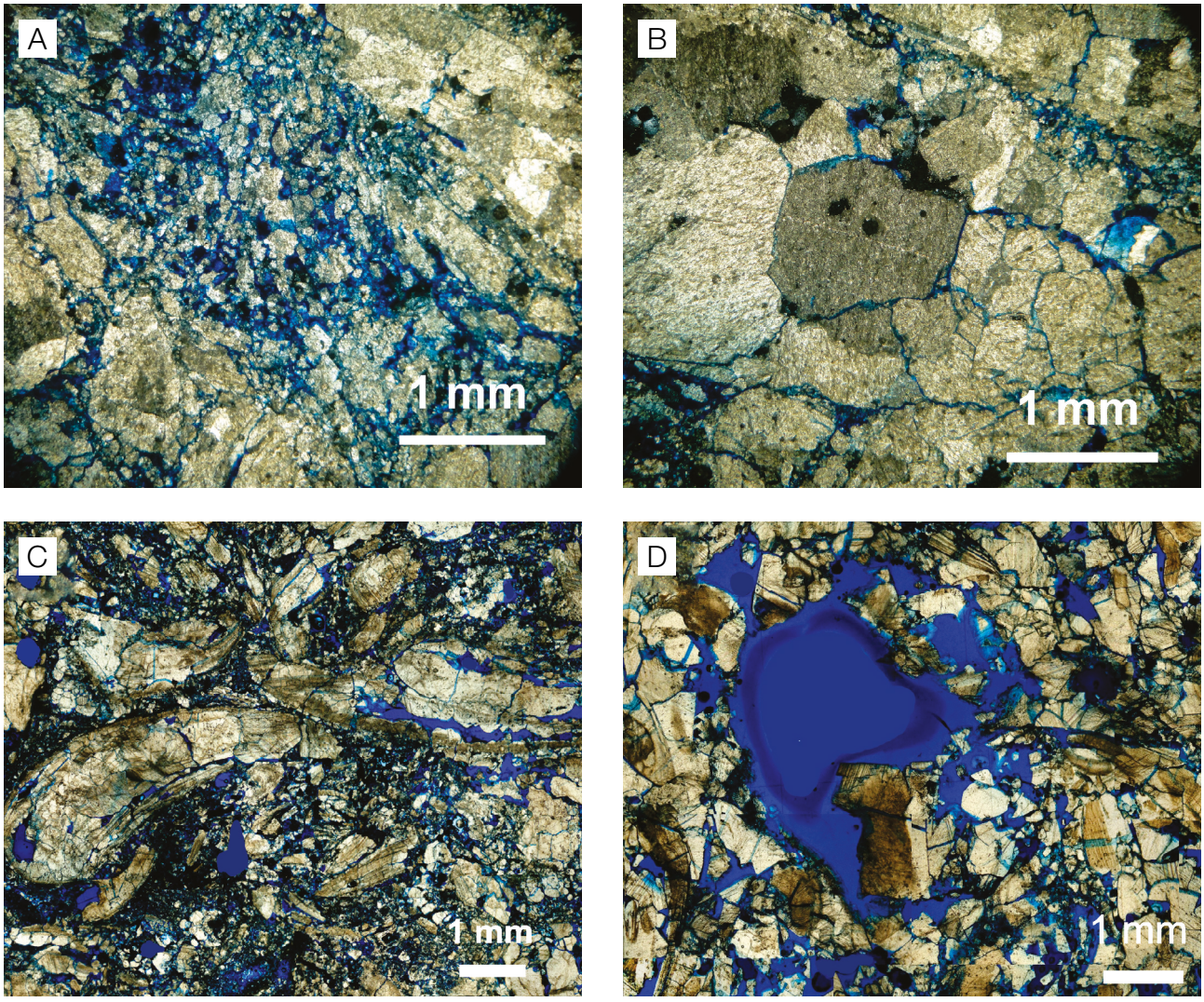

Figure 2. The different porosity types present in the selected samples. (A) Interparticle porosity between grains. (B) Interparticle porosity between crystals (intercrystalline). (C) Separate vugs (pores inside grains). (D) Touching vugs (connected network of vugs).

connected pores) was directly related to the permeability values obtained in the laboratory.

Table 1 shows that samples A1, A2 and C (Figure 4A1, A2 and C) have the highest permeabilities and the highest effective porosities, where sample B (Figure 4B) has low permeability and low effective porosity.

The 3D imaging of pore space (Figure 4) shows that the calcarenite (Figure 4A1) contains small pores (approximately 0.9 mm^3) regularly distributed throughout the rock. Using the effective porosity, it is possible to evaluate that 92% of pore space are connected in A1 (Figure 4A1). Calcirudite A2 (Figure 4A2) has large pores with average size of 1.4 mm^3 and 73% of its pores are connected.

The calcirudite B (Figure 4B) has a porosity of 10.87% and large pores (approximately 1.5 mm^3), however the permeability (0.86 mD) and connected pores (only 53%) are very low as a result of the isolated pores. Furthermore, this sample has horizontal lamination, which divides the rock in fine layers with different porosities depending on the material comprising each one. The highest porosity is associated with the layer consisting of calcirudite without matrix. The calcarenite layer contains siliciclastic matrix, which greatly decreases the porosity.

The calcirudite C (Figure 4C) presents touching vugs, in which the pores are connected by a very irregular network, which increases significantly the permeability—even though the porosity is somewhat smaller than A1 (Figure 4A1), the sample presents the higher permeability (52 mD) and 84% of connected pores.

Representative elementary volume

The determination of the REV is essential to validate the petrophysical analysis and is also a useful tool in the evaluation of rock heterogeneity.

In order to calculate the REV, five subvolumes were selected in different areas of the sample, increasing progressively the cube dimensions to evaluate the scale effect on the porosity value (Figure 5).

For each subvolume, the porosity values and variograms were calculated in three directions: x and y, orthogonal to each other and both on the horizontal plane, and z (depth) at a 90º angle with the horizontal plane (Figure 6).

The spatial continuity of variograms is associated with the sedimentary structures, which makes it relevant to perform this analysis at macro-scale to represent large structures

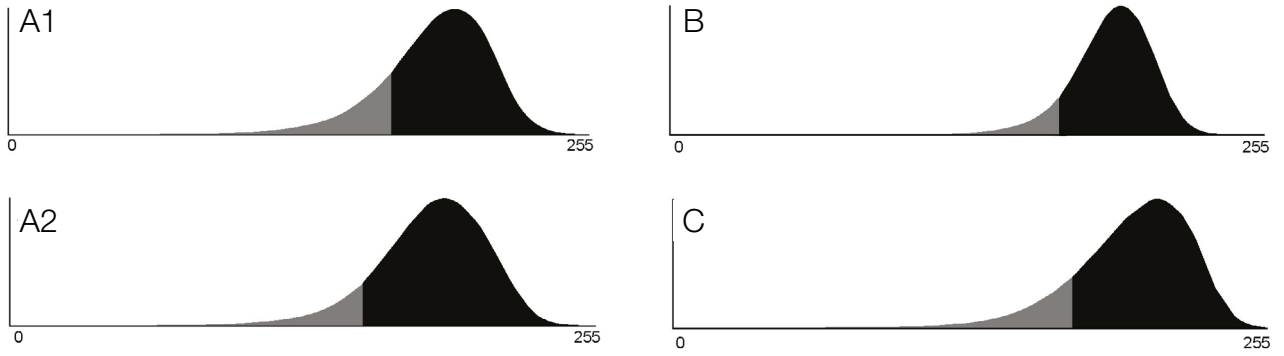

Figure 3. Histogram for the grayscale computed tomography (CT) images and the porosity threshold defined by self-organizing maps (SOM) segmentation for each sample (gray: pore; black: rock).

Table 1. Results obtained from laboratory and computed tomography/self-organizing maps (CT-SOM) data and the associated error.

			Laboratory data		Tomography data		
Sample	Rock classification	Pore space classification	Porosity (%)	Permeability (mD)	Porosity (%)	Effective Porosity (%)	Error (Lab./ CT-SOM) (%)
A1	Calcarenite	Interparticle	19.75	37.87	21.51	19.79	-8.9
A2	Calcirudite	Interparticle	14.36	37.77	12.49	9.09	13.0
B	Calcirudite	Separate vugs	10.32	0.86	10.87	5.79	-5.3
C	Calcirudite	Touching vugs	16.90	52.13	16.10	13.44	4.7

Lab.: laboratory.

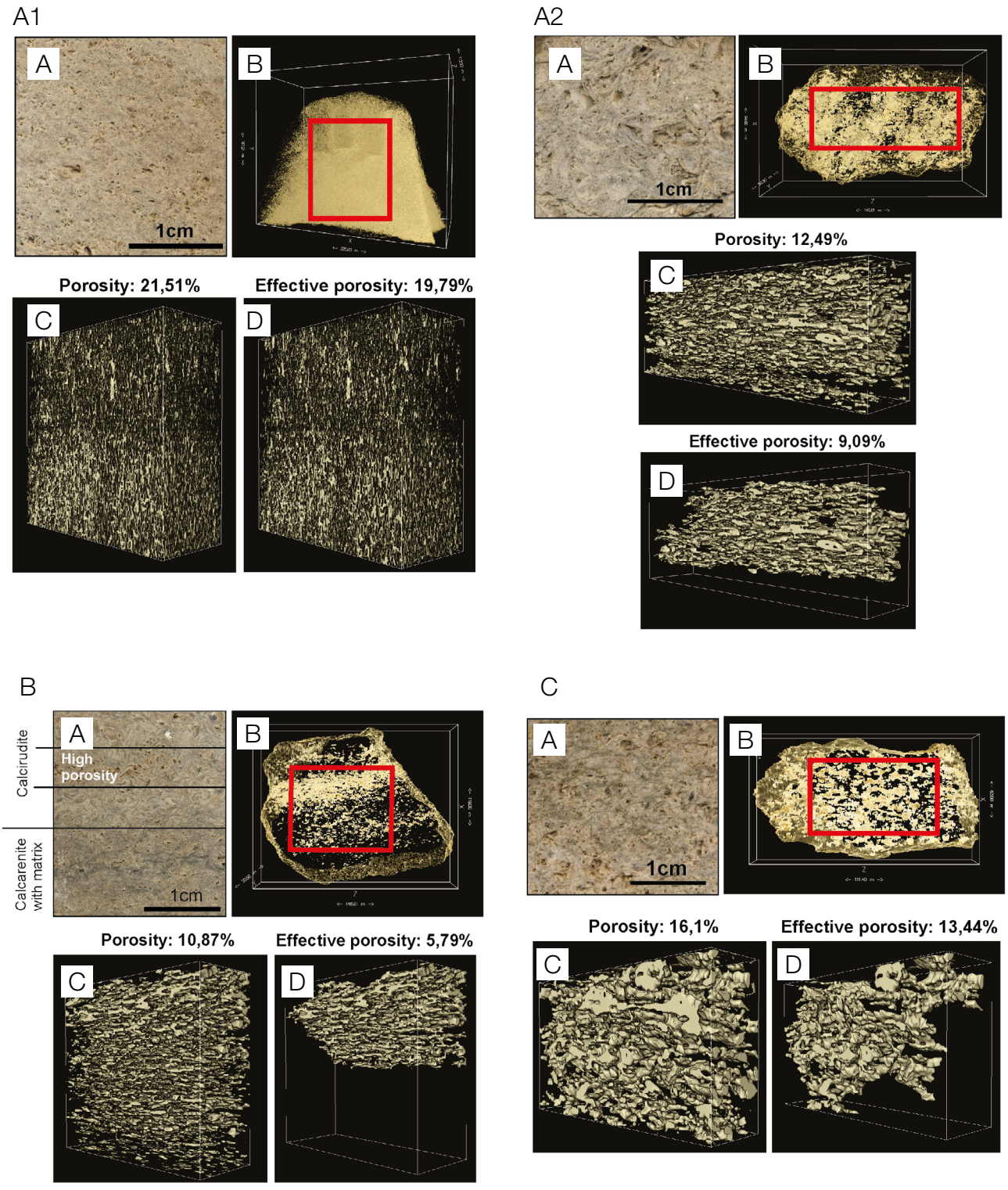

Figure 4. Pore space visualization for each sample. (A) Sample scanned image, the detail in sample B shows the variation of porosity in different layers (calcirudite with high porosity and calcarenite with matrix and low porosity); (B) three-dimensional (3D) view of total sample (in red the definition of the volume of interest—VOI); (C) total porosity in the volume of interest; (D) effective porosity (connected pores) in the volume of interest.

such as vertical and lateral variations. Furthermore, the degree of correlation, which is calculated in the variogram as the sill value, is directly related to the number of samples required to calculate the rock property. This occurs because the greater degree of correlation means that the samples are similar, thus a few samples would be necessary to represent the overall rock property (Rautman, 1991). In this way, the spatial correlation shown in the variogram also relates to the representative elementary volume, once the REV is the minimum volume necessary to represent the overall rock property.

The variograms of smaller volumes have short continuity and a non-constant sill, because the sample volume is below the rock heterogeneity scale. As the volumes increase, the sill becomes stable, indicating the data stationarity. Indeed, data correlation depends only on the distance between the points and not on their location, which was demonstrated by the same porosity values obtained for the different regions V1, V2, V3, V4 and V5.

The results reveal that increasing the sampling volume the porosity values reduce dispersion and present stationary behavior. Thus, it is possible to determine REV for the porosity parameter from which the porosity measurements, for different areas, have little or no variation and approach the overall value (Figure 6).

It is also possible to infer the REV from the variogram parameters as the volume in which the data becomes stationary, *i.e.*, the heterogeneity scale is representative of the overall heterogeneity (Figure 6). Therefore, both ways of determining REV allow a better control of the heterogeneity evaluation.

Table 2 shows the REV obtained for the four samples.

The spatial continuity of variograms is associated with the spatial rock structures. Thus, in these samples, spatial continuity is related mainly to the pore size: the calcarenite with interparticle porosity has the lowest range, and the calcirudite with touching vugs has the highest range, indicating the most heterogeneous pore space distribution.

The lowest REV calculated corresponds to the calcarenite (Figure 6A1). This sample presents little dispersion of porosity values even in small volumes as a result of the homogeneous pore distribution and little vertical and horizontal variations in addition to the small particles (< 2 mm) and pores (0.9 mm^3).

The calcirudite presenting interparticle porosity (Figure 6A2) and the calcirudite with separate vugs (Figure 6B) show intermediate REV volumes (Table 2). These samples present large particles (> 2 mm) and pores (between 1.4 and 1.5 mm^3), which affect the rock heterogeneity since the spatial continuity depends on the spatial structures scale. Moreover, in sample B (Figure 6B) the sedimentary structures of deposition roots the rock anisotropy, which can be seen in the variogram by the different sills in directions x, y and z.

At last, the calcirudite with touching vugs (Figure 6C) presents the largest REV related to the highest pore space heterogeneity. In this sample, in addition to the large pores (1.7 mm^3) the very irregular network connecting the vugs also contributes to increase the rock heterogeneity.

The results show that a small volume is required to obtain a representative volume of the overall pore distribution in the studied samples, with the maximum value of 12 cm^3, which is approximately equivalent to a small plug of 1" in diameter per 2,5 cm of height (Table 2).

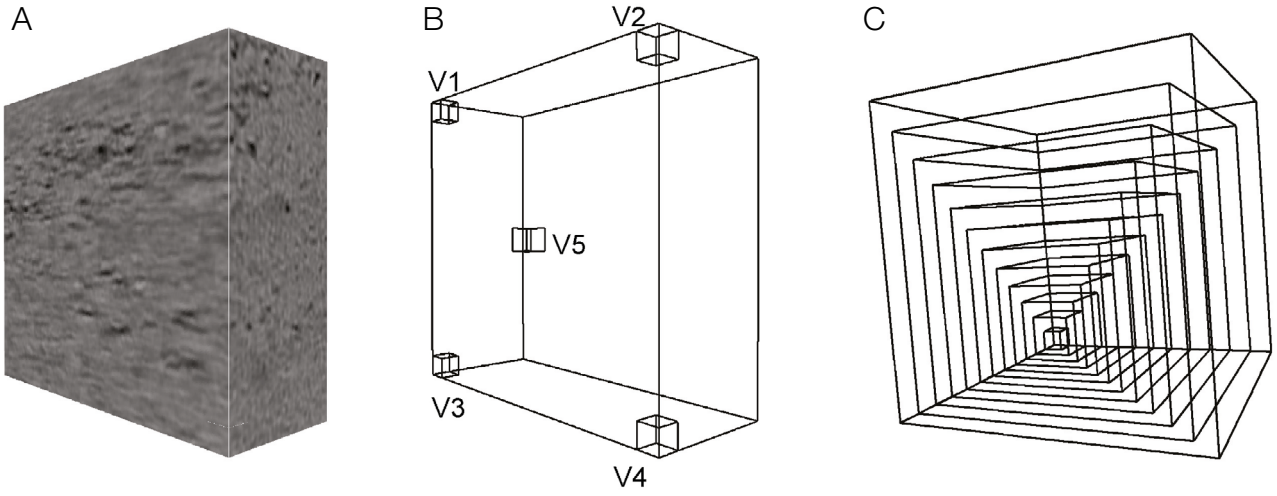

Figure 5. Sampling for the representative elementary volume calculation: (A) total volume of interest in grayscale imaging; (B) the definition of the five initial subvolumes V1, V2, V3, V4 and V5; (C) detail of the progressive increase of volume in each subvolume.

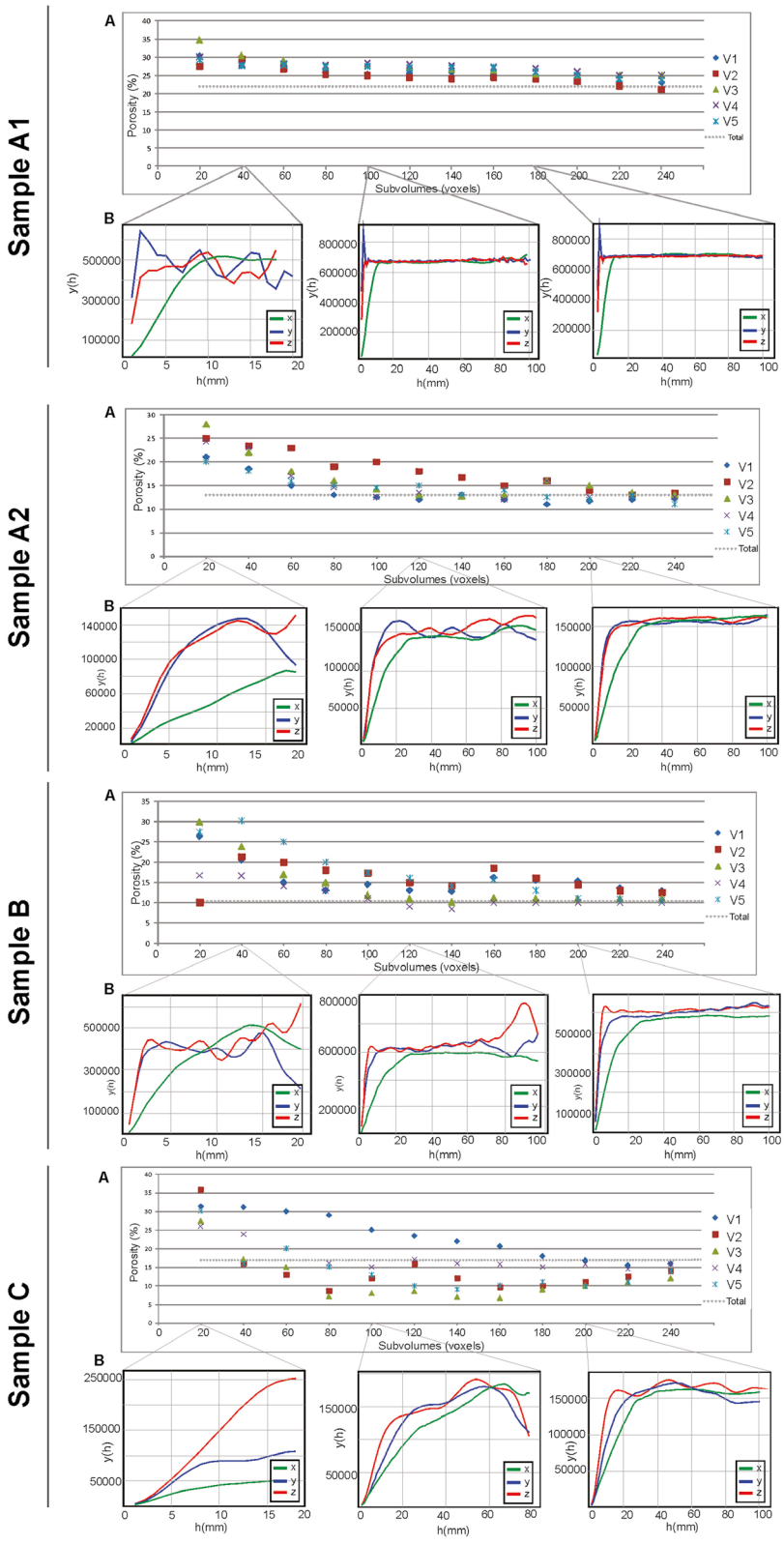

Figure 6. Comparison between the definition of the representative elementary volumes for samples A1, A2, B and C: (A) porosity values for increasingly subvolumes in different localizations (V1: upper left; V2: upper right; V3: bottom left; V4: bottom right; V5: center; Total: total sample volume). (B) Variograms in three directions (x, y and z) for different subvolumes.

Table 2. Representative elementary volumes (REV) for each sample.

Samples	Rock classification	Pore space classification	REV (cm^3)	REV (% of VOI)
A1	Calcarenite	Interparticle	3.7	1.1%
A2	Calcirudite	Interparticle	5.8	7.6%
B	Calcirudite	Separate vugs	5.4	9.3%
C	Calcirudite	Touching vugs	12.1	51.4%

CONCLUSIONS

CT is an effective tool in 3D pore space characterization, capable of providing not only the porosity and connectivity values, but also as an input to the evaluation of heterogeneity by variogram and REV analyses. The segmentation of CT data by the algorithm based on the SOM technique for 3D volumes proved to be a consistent method for image segmentation.

In addition, as demonstrated by our results, REV calculation contributes to reduce data computational processing and to perform reliable analyses at laboratory scale.

The pore space heterogeneity is controlled by lateral and vertical variations, which can be analyzed by the variograms in different directions. It is possible to characterize the rock heterogeneity, as well as the anisotropy.

Integrating the petrographic and heterogeneity analysis, such as REV and variography, it is possible to relate micro to macroscales features. The cement dissolution is the mainly diagenetic process that controls the present pore space. The dissolution can result in vugs and interparticle pores depending on two main factors: grain size and packing. Grain size is a result of sedimentation, while packing is a combination between sedimentation and diagenesis, once compactation might heavily modify the rock structure. Furthermore, increasing density of packing results in interparticle porosity and smaller pores, while a loose packing tend to originate larger pores. Another factor that can affect pore space heterogeneity, specially the vertical variability, is the horizontal laminations, as demonstrated in the analysis of sample B (Figure 4B).

Although there are many factors controlling the pore space heterogeneity, a detailed description may help understanding the configuration of pore distribution and how it relates to the petrophysical properties.

REFERENCES

Al-Raoush, R., Papadopoulos, A. (2010). Representative elementary volume analysis of porous media using x-ray computed tomography. *Powder Technology*, 200(1-2), 69-77. https://doi.org/10.1016/j.powtec.2010.02.011

Arns, C. H., Bauget, F., Limaye, A., Sakellariou, A., Senden, T. J., Sheppard, A. P., Sok, R. M., Pinczewski, V., Bakke, S., Berge, L. I., Oren, S. E., Knackstedt, M. A. (2005). Pore-scale characterization of carbonates using X-ray microtomography, *Society of Petroleum Engineers Journal*, 10(4), 475-484. https://doi.org/10.2118/90368-PA

Arzuman S. (2009). *Comparison of Geostatistics and Artificial Neural Networks in Reservoir Property Estimation*. Thesis (Doctorate). Ankara Eskisehir: Geological Engineering Departament, Middle East Technical University. 162 p.

Azambuja Filho, N. C., Arienti, L. M., Cruz, F. E. G. (1998). Guidebook to the Rift-Drift Sergipe-Alagoas Passive Margin Basin, Brazil. *AAPG International Conference & Exibition*, Rio de Janeiro.

Bear, J. (1972). *Dynamics of fluids in porous media*. New York: American Elsevier Publishing Co. 483 p.

Bhatt, A., Helle, H. B. (2002). Determination of facies from well logs using modular neural networks. *Petroleum Geoscience*, 8(3), 217-228. https://doi.org/10.1144/petgeo.8.3.217

Castro, P. T. A. (1988). *Fatores que Controlam a Deposição nas Coquinas nas Sequências Rifte em Bacias da Margem Leste Brasileira*. Dissertação (Mestrado). Ouro Preto: Programa de Pós-graduação em Geologia – UFOP.

Coléou, T., Poupon, M., Azbel, K. (2003). Unsupervised seismic facies classification: A review and comparison of techniques and implementation. *The Leading Edge*, 22, 942-953. https://doi.org/10.1190/1.1623635

Corbett, P. W. M., Jensen, J. L. (1992). Variation of reservoir statistics according to sample spacing and measurement type for some intervals in the Lower Brent Group. *The Log Analyst*, 33, 22-41.

Fernandes, J. S., Appoloni, C. R., Fernandes, C. P. (2012). Determination of the representative elementary volume for the study of sandstones and siltstones by x-ray microtomography. *Materials Research*, 15(4), 662-670. http://dx.doi.org/10.1590/S1516-14392012005000081

Figueiredo, A. M. F. (1981). *Depositional Systems in the Lower Cretaceous Morro do Chaves and Coqueiro Seco Formations, and their Relationship to Petroleum Accumulations, Middle Rift Sequence, Sergipe–Alagoas Basin, Brazil*. Thesis (Doctorate). Austin: University of Texas. 275p.

Grabau, A. W. (1904). The Classification of Sedimentary Rocks. *American Geologist*, 33, 228-247.

Hulea, I. N., Nicholls, C. (2012). Carbonate rock characterization and modeling–Capillary pressure and permeability in multimodal rocks. *AAPG Bulletin*, 96(9), 1627-1642. https://doi.org/10.1306/02071211124

Ketcham, R. A., Carlson, W. D. (2001). Acquisition, optimization and interpretation of x-ray computed tomographic imagery: applications to the geosciences. *Computers & Geosciences*, 27(4), 381-400. http://dx.doi.org/10.1016/S0098-3004(00)00116-3

Kohonen, T. (2001). *Self-organizing maps*. New York: Springer-Verlag. 501p.

Li, Y., Chi, Z. (2005). MR Brain Image Segmentation Based on Self- Organizing Map Network. *International Journal of Information Technology*, 11(8).

Lie, J., Lysaker, M., Tai, X. C. (2006). A variant of the level set method and applications to image segmentation. *Mathematics of Computation*, 75(255), 1155-1174.

Lonoy, A. (2006). Making sense of carbonate pore systems. *AAPG Bulletin*, 90(9), 1381-1405. https://doi.org/10.1306/03130605104

Lucia, F. J. (1983). Petrophysical parameters estimated from visual descriptions of carbonate rocks: a field classification of carbonate pore space. *Journal of Petroleum Technology*, 35, 629-637. https://doi.org/10.2118/10073-PA

Lucia, F. J. (2007). *Carbonate Reservoir Characterization*. 2ª ed. New York: Springer-Verlag. 226p.

Lucia, F. J., Fogg, G. E. (1990). Geologic/Stochastic Mapping of Heterogeneity in a Carbonate Reservoir. *Journal of Petroleum Technology*, 42(10), 1298-1303.

Mei, P. A., Carneiro, C. C., Kuroda, M. C., Fraser, S. J., Min, L. L., Reis, F. (2017). Self-Organizing Maps as a Tool for Segmentation of Magnetic Resonance Imaging (MRI) of Relapsing- Remitting Multiple Sclerosis. *12th International Workshop on Self-Organizing Maps and Learning Vector Quantization, Clustering and Data Visualization (WSOM)*, p. 1-7. Nancy.

Nordahl, K., Ringrose, P. S. (2008). Identifying the representative elementary volume for permeability in heterolithic deposits using numerical rock models. *Mathematical Geosciences*, 40(7), 753-771. https://doi.org/10.1007/s11004-008-9182-4

Oh, W., Lindquist, W. B. (1999). Image thresholding by indicator Kriging. *IEEE Transactions on Pattern Analysis and Machine Intelligence*, 21(7), 590-601. https://doi.org/10.1109/34.777370

Okabe, H., Blunt, M. J. (2007). Pore space reconstruction of vuggy carbonates using microtomography and multiple point statistics. *Water Resources Research*, 43, W12S02. https://doi.org/10.1029/2006WR005680

Otsu, N. (1979). A threshold selection method from gray-level histograms. *IEEE Transactions on Systems, Man, and Cybernetics*, 9(1), 62-66. https://doi.org/10.1109/TSMC.1979.4310076

Rautman, C. A. (1991). Estimates of Spatial Correlation in Volcanic Tuff, Yucca Mountain, Nevada. *Sandia Report*, SAND89-2270, 110 p.

Razavi, M. R., Muhunthan, B., Al Hattamleh, O. (2007). Representative elementary volume analysis of sands using x-ray computed tomography. *ASTM Geotechnical Testing Journal*, 30(3), 212-219. https://doi.org/10.1520/GTJ100164

Reis Neto, J. M., Fiori, A. P., Lopes, A. P., Marchese, C., Pinto-Coelho, C. V., Vasconcellos, E. M. G., Silva, G. F., Secchi, R. (2011). A microtomografia computadorizada de raios x integrada à petrografia no estudo tridimensional de porosidade em rochas. *Revista Brasileira de Geociências*, 41(3), 498-508.

Ridler, T. W., Calvard, S. (1978). Picture thresholding using an iterative selection method. *IEEE Transactions on Systems, Man, and Cybernetics*, SMC-8(8), 630-632. https://doi.org/10.1109/TSMC.1978.4310039

Sahin, A., Ghori, S., Ali, A., El-Sahn, H., Hassan, A., Al-Sanounah, A. (1998). Geological controls of variograms in a complex carbonate reservoir, eastern province, Saudi Arabia. *Mathematical Geology*, 30(3), 309-322. https://doi.org/10.1023/A:1021780915406

Tidwell, V. C., Wilson, J. L. (1997). Laboratory method for investigating permeability upscaling. *Water Resources Research,* 33(7), 1607-1616. https://doi.org/10.1029/97WR00804

Van Geet, M., Lagrou, D., Swennen, R. (2003). Porosity measurements of sedimentary rocks by means of microfocus X-ray computed tomography. In: F. Mees, R. Swennen, M. Van Geet, P. Jacobs (Eds.), *Applications of X-ray Computed Tomography in the Geosciences* (215, 51-61). London: Geological Society, Special Publications.

Vik, B., Bastesen, E., Skauge, A. (2013). Evaluation of representative elementary volume for a vuggy carbonate rock—Part: Porosity, permeability, and dispersivity. *Journal of Petroleum Science and Engineering*, 112, 36-47. https://doi.org/10.1016/j.petrol.2013.03.029

Vincent, B., Fleury, M., Santerre, Y., Brigaud, B. (2011). NMR Relaxation of Necritic Carbonates: An Integrated Petrophysical and Petrographical Approach. *Journal of Applied Geophysics*, 74, 38-58. https://doi.org/10.1016/j.jappgeo.2011.03.002

Vogel, J. R., Brown, G. O. (2003). Geostatistics and the representative elementary volume of gamma ray tomography attenuation in rock cores. In: F. Mees, R. Swennen, M. Van Geet, P. Jacobs (Eds.), *Applications of X-ray Computed Tomography in the Geosciences* (215, 81-93). London: Geological Society, Special Publications. https://doi.org/10.1144/GSL.SP.2003.215.01.08

Wang, F. P., Lucia, F. J., Kerans, C. (1994). Critical scales, upscaling, and modeling of shallow-water carbonate reservoirs. *Society of Petroleum Engineers*, SPE 27715, 765-773. https://doi.org/10.2118/27715-MS